Plasma effects on harmonic spectra generated from moderately relativistic laser-plasma interactions

R. Ondarza-Rovira[1] and T. J. M. Boyd[2]

[1]*Instituto Nacional de Investigaciones Nucleares, Apartado Postal 18-1027, México 11801, Distrito Federal, Mexico*

[2]*Centre for Theoretical Physics, University of Essex, Wivenhoe Park, Colchester CO4 3SQ, Essex, United Kingdom*

(Received 16 March 2012; revised manuscript received 7 August 2012; published 29 August 2012)

When intense p-polarized laser light is incident on a plasma with an electron density many times the critical density, the flux of fast electrons created by Brunel absorption excites plasma oscillations. These oscillations may in turn affect the spectrum of high harmonics by modulating the spectrum at the plasma frequency, ω_p, and by coupling to the radiation field through the steep density gradient at the plasma-vacuum interface, so generating *plasma line emission* (PLE) at ω_p and harmonics of ω_p. Both aspects depend sensitively on a range of plasma and laser pulse parameters, including the initial electron density, the density profile at the plasma-vacuum interface, and the intensity, pulse shape, and pulse length of the incident laser light. These various dependences have been characterised for moderately relativistic laser-plasma interactions by means of a series of particle-in-cell (PIC) simulations.

DOI: 10.1103/PhysRevE.86.026407 PACS number(s): 52.38.Dx, 42.65.Ky, 52.65.Rr

I. INTRODUCTION

Radiation generated in plasmas at harmonics of some fundamental frequency is generally a signature of nonlinear interactions in the plasma source, and as such offers diagnostic potential both in laboratory and naturally occurring plasmas. Recently, a good deal of attention has been paid to radiation from plasma sources created by the interaction of intense laser light with solid density targets such that the plasma is overdense in terms of the critical density. This has prompted a renewal of interest in effects well known from more benign regions of parameter space. One of the most enduring of these is the generation of high harmonics of the incident laser light.

The first observation of multiple harmonics from laser-plasma interactions was reported as long ago as 1977 [1,2]. Burnett *et al*. [1] recorded harmonics up to the 11th from the irradiation of solid targets with long-pulse (2 ns) CO_2 laser light. In later experiments at significantly higher irradiances, typically $I \sim 3 \times 10^{16}$ W cm^{-2}, Carman and his associates detected harmonics up to the 46th from targets irradiated with CO_2 light [3,4]. These spectra were interpreted by Bezzerides, Jones and Forslund [5], who showed that high harmonic generation was a consequence of nonlinear resonant absorption in a steepened density profile.

With neodymium glass lasers supplanting CO_2 systems, the corresponding hundredfold reduction in values of $I\,\lambda_L^2$, where λ_L denotes the wavelength of the incident light, meant that the harmonic orders recorded by Carman *et al*. were not surpassed until the availability of short-pulse systems restored levels of $I\,\lambda_L^2$ to those attained more than a decade earlier [6–8]. Norreys *et al*. [8], using 2.5 ps pulses of Nd:laser light at intensities of 10^{19} W cm^{-2}, resolved harmonics up to the 68th, with harmonic power decaying only slowly with harmonic number m and with power efficiencies $P_m/P_1 \gtrsim 10^{-6}$.

From particle-in-cell (PIC) simulations of harmonic generation at these intensities Gibbon [9] found empirically that the efficiency of high-order harmonic generation η_m scales as $\eta_m \sim 9 \times 10^{-5}\,(I_{18}\,\lambda_L^2)^2 \times (m/10)^{-5}$ where I_{18} denotes light intensity in units of 10^{18} W cm^{-2}; m is the harmonic number and λ_L is the wavelength in microns. Good agreement was found between Gibbon's scaling law and the efficiency scaling of the measured spectra except at the highest value of $I\,\lambda_L^2 = 10^{19}$ W μm^2 cm^{-2} where the decay index is closer to 3 than to 5.

Whereas target plasmas in early experiments were characterized by scale lengths $L > \lambda_L$, so allowing coupling of an electromagnetic wave into a localized electrostatic mode at the critical density n_c by means of resonance absorption to function effectively, this becomes increasingly less efficient in the short-pulse regime. With pulse lengths of a few hundred femtoseconds, plasma scale lengths shorten to give a steep plasma-vacuum interface so that conditions for mode conversion become less and less favorable. Physically, in a steepened density profile the Langmuir wave electric field is no longer resonantly excited to levels $E_L(c\,/\,V_e)^{1/2}$, where V_e denotes the electron thermal velocity, but for $a_0 \gtrsim 1$ [where $a_0 \sim 0.85\,(I_{18}\lambda_L^2)^{1/2}$ denotes the normalized quiver momentum] it remains comparable to the incident field E_L.

Conveniently for harmonic generation, as a_0 increases and electron dynamics become increasingly relativistic, alternative sources come into play; in particular, interest has been focused on $(\boldsymbol{v} \times \boldsymbol{B})$-driven harmonic generation [10–14]. In what has come to be known as the oscillating mirror model, OMM for short, incident laser light is reflected from an oscillating plasma density surface, modeled as a step profile, motion that gives rise to a phase modulation with the spectrum of the reflected light showing sidebands at harmonics of the laser frequency. The detailed interaction physics is disregarded and represented phenomenologically by the oscillation of the overdense plasma surface at a frequency twice that of the incident laser, corresponding to the ponderomotive force. In practice, in order to reconcile the model with PIC simulations it was found necessary to include additional modes excited by nonlinear coupling [13].

As an adjunct to a more complete understanding of high-harmonic generation, HHG, consideration needs to be given to that part of the nonlinear current source *not* taken into account in the OMM, namely, the contribution that derives from density compression. Our early work [15] emphasised the role of plasma effects on the harmonic spectrum, in particular

plasma line emission, PLE for short, as well as a modulation of the spectrum in the shape of what we called a "combination line" [16]. Following evidence of modulated spectra presented by Teubner *et al.* [17], Boyd and Ondarza-Rovira repeated earlier PIC simulations over an extended harmonic range and found evidence of modulation of the spectrum at the plasma frequency [18,19].

This paper brings together hitherto unpublished data supporting our contention that PLE and plasma modulation may, for suitable choices of parameters, affect the high-harmonic spectrum. We consider here interactions in a *moderately relativistic* range, one which we identify, albeit arbitrarily, as $0.5 \lesssim a_0 \lesssim 5.0$. Whereas our earlier published spectra mainly reflected the dependence on a_0 and n_{e0}/n_c, where n_{e0} denotes the initial electron density, we explored other key parametric dependences of both the reflected and transmitted spectra. These included not only pulse length and shape, but the density scale length at the front of the plasma and the electron temperature, T_e. In Sec. II we review briefly some details of the PIC model, along with aspects of Brunel excitation of the plasma line and of plasma line emission. Section III considers the effects of the growing Langmuir wave in modulating the spectrum before emission at the plasma frequency becomes a dominant feature of the spectrum as growth saturates. Further consideration is given to the effect of variation of the electron temperature as well as Brunel-induced plasma wave excitation *across* the density ramp. Although we made reference to the latter in our earlier work [15,16], the emphasis there was on plasma effects at the peak plasma electron density, n_{e0}. In Sec. IV we consider the effect of the same parametric dependences discussed in Sec. III on plasma modulation of the spectrum. Our conclusions are summarized in Sec. V.

II. PLASMA LINE EMISSION

Radiation at the plasma frequency has a long history in plasma physics, identified from sources as varied as gas discharges [20], stellarators [21], the aurora [22], and solar corona [23,24]. In whatever context, the requirements for emission at the plasma frequency are twofold. First an electron beam is needed to excite suprathermal levels of Langmuir waves, followed by effective coupling of these to the radiation field [25]. By and large, Langmuir wave excitation is better understood than the coupling phase. Given that electron beams or jets and plasma density gradients are commonplace in plasmas both natural and manmade, it is hardly surprising that radiation from plasma oscillations is present to some degree in many sources. However, coupling to the radiation field is often not sufficiently strong for plasma emission to be significant in practice.

Conditions favorable for both excitation and coupling phases are found in some laser-produced plasmas. Inverse resonance absorption has been shown to contribute to plasma emission from inhomogeneous plasmas with an efficiency of up to ~60%, predicted from a theoretical model and confirmed by PIC simulations [26]. Radiation at the second harmonic was also detected, attributable to two Langmuir waves coupling to produce radiation at $2\omega_p$ through inverse two-plasmon decay. High-intensity laser interactions with dense plasmas provide an environment that is in a sense tailor made for plasma emission. Langmuir waves are driven to suprathermal levels by the flux of fast electrons penetrating the supradense plasma beyond the critical density so that the plasma radiation generated appears at frequencies well above that of the incident light.

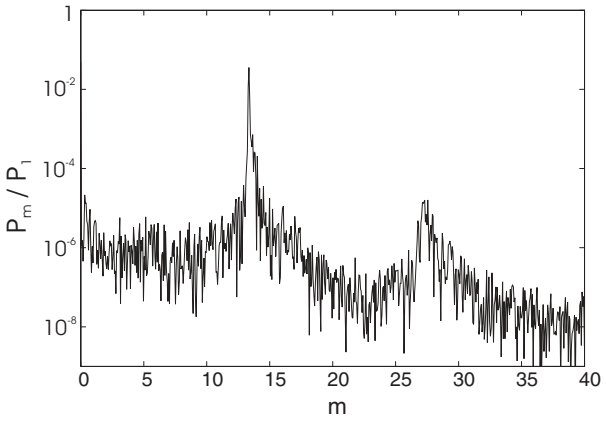

FIG. 1. Post-pulse plasma emission at ω_p and $2\omega_p$ for $n_{e0}/n_c = 200$ and $a_0 = 2.0$; $m = \omega/\omega_L$. Emission in the plasma lines is normalized to the power initially incident on the plasma.

The issue of plasma emission was revisited by Boyd and Ondarza-Rovira [15,16] in PIC simulations of the interaction of moderately intense laser light with plasmas of density up to 200 times critical density. Figure 1 shows emission at the plasma frequency and its second harmonic from a PIC simulation with $a_0 = 2.0$, $n_{e0}/n_c = 200$, at a time after the end of the laser pulse, so that harmonics of the laser light are no longer present in the spectrum. The plasma emission is normalized to the incident power.

The physics of high-harmonic generation has been comprehensively reviewed by Teubner and Gibbon [27], who have discussed not only mechanisms responsible for harmonic emission but its characterization in terms of laser and plasma parameters.

A. Particle-in-cell model

Lacking any credible fully self-consistent theory of plasma emission under the conditions of intense laser interaction with supradense plasmas at a plasma-vacuum interface, our best hope of gaining insight into the phenomenon lies with PIC simulations across a range of parameters.

We have not attempted to model the ionization of target material but treat instead the interaction of a laser pulse of length t_p with a plasma slab of initially uniform density, apart from an interface at the front end. This vacuum-plasma interface is characterized by a density profile with scale length Δ that is some prescribed fraction of a wavelength across the ramp. We have used a one and a half dimension (1-1/2D) fully relativistic and explicit PIC code, that embeds the Bourdier technique [28] to allow for oblique incidence. Two vacuum gaps extend from both the front of the ramp and the planar rear surface of the plasma to the walls of the simulation box to allow for particle and wave propagation. When external fields reach the boundary and propagate outside the system they are not reflected and thus no longer considered in the interaction physics.

Plasma particles are reflected at the boundaries by reversing their velocities. The plasma filled a simulation box extending over four laser wavelengths with 2×10^6 particles distributed across 10^4 grids, giving a ratio of grid size to wavelength of $\sim 10^{-4}$. The number of particles employed and the choice of the simulation parameters is sufficient to resolve both the Debye length and the highest frequency mode with acceptable resolution.

The initial electron temperature was chosen to be 100 eV, apart from cases where the effect of electron temperature on the harmonics was investigated. Gaussian pulses of variable length and profile have been used. Ions were treated as a neutralizing immobile background, an acceptable approximation given the femtosecond time scales governing these simulations, where typically Gaussian pulses of duration 10–100 fs have been used throughout. The laser parameter a_0 lies in the moderately relativistic range (0.5–5.0), with plasma densities up to $200n_c$. The reflected emission spectra showing the relative strength of the different oscillation modes are determined from a time-resolved Fourier decomposition of the harmonic contents of the reflected electric field at the vacuum gap, normalized to the fundamental.

B. Plasma line emission (PLE) and modulation

We review briefly results from a set of simulations carried out with moderately intense p-polarized light ($a_0 = 0.5$–2.0) incident on plasma slabs in which the initial electron density, n_{e0}, was varied from $n_{e0}/n_c = 30$ to 200 [16]. The principal characteristics of the spectra reported were as follows:

(i) For the chosen pulse length, the spectrum in Fig. 2(a) shows plasma emission at $m_p = \omega_p/\omega_L = (n_{e0}/n_c)^{1/2} \sim 5.5$ as a dominant feature, comparable in intensity to the power radiated in the third harmonic. The spectrum is distinct from the roll-off spectra found from simulations characterized by both higher laser intensity and lower initial plasma density [9]. That combination sets any plasma emission in the range of comparatively high-intensity low harmonics in the spectrum of reflected light with the result that the plasma line is to some extent masked.

(ii) As well as plasma emission at the peak electron density, PLE, in practice additional emission appears at normalized frequencies $m = 2,3,\ldots$ up to $(n_{e0}/n_c)^{1/2}$; cf. Ref. [16]. However, as plasma emission scales as the square of the electron density, low ($\boldsymbol{v} \times \boldsymbol{B}$)-driven laser harmonics often dominate this region of the spectrum.

(iii) The other distinctive aspect of the spectrum in Fig. 2(a) is the modulation that appears on the blue side of the plasma line with intensity an order of magnitude below that of the plasma line. This unexpected spectral detail proved to be a robust feature for the range of parameters simulated. At the time we referred to it as the *combination line*, a label intended to identify the feature as one reflecting properties of both the plasma source and laser harmonics across the density ramp at the front end of the plasma box. In Fig. 2(a) the modulation is centered at $m_c = 3 + m_p$ and of width $\Delta m \sim 3$.

(iv) The spectrum shown in Fig. 2(b), for $n_{e0}/n_c = 64$ so that $\omega_p/\omega_L = 8$ exactly, shows some similarities to the pattern found in Fig. 2(a), but also some differences. While a footprint of the combination line persists, what is distinctive about the spectrum in Fig. 2(b) is the modulation of harmonics ($m = 8 = m_p$ to $m = 12$).

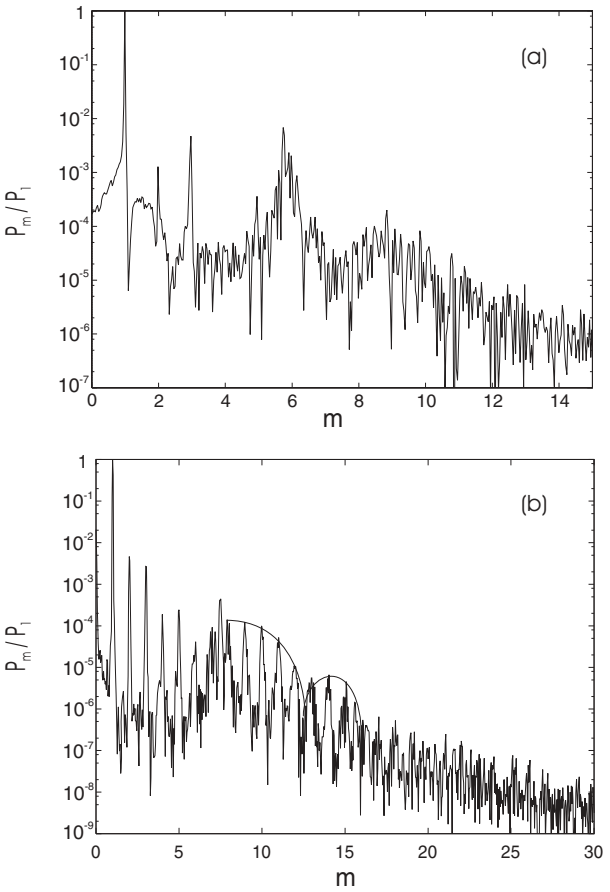

FIG. 2. (a) Normalized harmonic spectrum showing laser harmonics in reflection and plasma line emission (PLE) at $m_p = (\omega_p/\omega_L) \sim 5.5$ for $n_{e0}/n_c = 30, a_0 = 0.5$, and (b) at $m_p = 8$ for $n_{e0}/n_c = 64, a_0 = 0.5$.

(v) For transmission spectra no combination feature was observed, consistent with the absence of lines with $m < m_p$ in transmission.

(vi) Electron trajectories were tracked entering the target plasma and Langmuir waves generated at the front of the plasma slab, recorded for different combinations (a_0,n_{e0}/n_c). This localization is important for the subsequent coupling of the plasma oscillations to the radiation field by means of the density gradient in the (perturbed) peak density region [16]. Figure 3 shows a representation of electron density across a section of the plasma target illuminated by p-polarized light incident at 23 degrees to the normal to the target surface, in the form of a contour plot. The parameter choices in Fig. 3 span the moderately relativistic range considered in this paper, ($a_0 = 0.5$, $a_0 = 5.0$); both show clear structure in electron density corresponding to the excitation of plasma oscillations. The plasma-vacuum interface is initially at $x = 0$. For the combination $a_0 = 0.5$ and $n_{e0}/n_c = 20$, $L/\lambda_L \sim 0.06$ while for $a_0 = 5.0$ and $n_{e0}/n_c = 100$, $L/\lambda_L \sim 0.08$; here L denotes the density scale length. In Fig. 3(a) $\tau_p/\tau_L \sim 0.2$, while for Fig. 3(b) $\tau_p/\tau_L \sim 0.1$, where τ_p denotes the plasma period and τ_L that of the incident light.

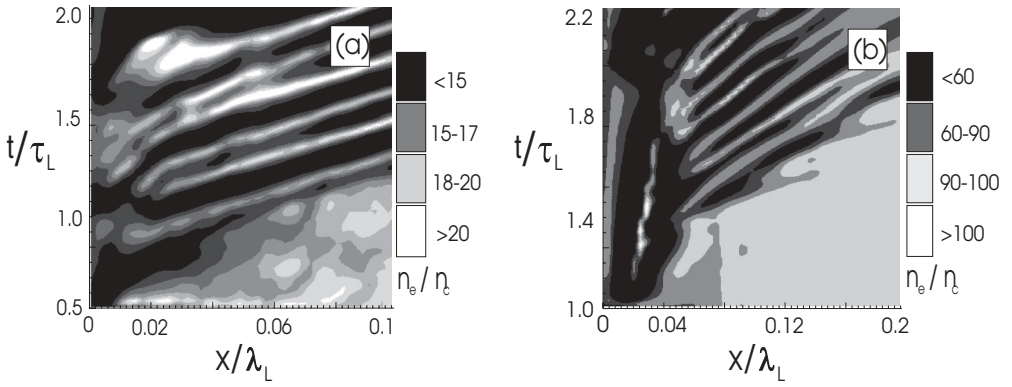

FIG. 3. (a) Plasma electron density structure close to the plasma-vacuum interface for a target plasma density $n_{e0}/n_c = 20$, $a_0 = 0.5$, recorded over 1.5 laser periods; the section of plasma shown extends over 0.1 λ_L [19]; (b) corresponding structure for the combination $n_{e0}/n_c = 100$, $a_0 = 5$, over 1.2 laser periods.

C. Brunel injection

Essential for the generation of PLE is a source of energetic electrons to drive Langmuir waves in the first place. In the case of radio bursts from the Sun, suprathermal electrons from solar flares drive Langmuir waves in the solar corona, while for laser-irradiated plasmas an equivalent source is at hand. As the intensity of the incident light increases, the nature of its absorption in the laser-plasma interaction changes as density gradients steepen. Resonance absorption becomes less effective and is supplanted by the mechanism first proposed by Brunel and called by him "not-so-resonant" resonant absorption [29], where electrons oscillating across a steep density gradient give rise to strong absorption. In the Brunel model, electrons are accelerated by the laser electric field at the surface, but are not considered subject to any field inside the plasma so that the analysis is not self-consistent.

Like resonant absorption, the Brunel mechanism too requires that the incident light be p-polarized and so depends on the angle of incidence. The angular dependence of Brunel absorption differs from the Denisov dependence for resonant absorption with distinct behavior in the limits of $a_0 < 1$, $a_0 \gg 1$ [30,31]. Most of the simulations reported here have been done with $\theta = 23^\circ$. While this choice is well below the optimum for Brunel excitation of Langmuir waves, it suits our present purpose well enough. Figure 4 shows that the efficiency of Brunel absorption recorded over sets of PIC runs increases more or less linearly across a range $1 \leqslant a_0 \leqslant 4$ before saturating. The range of linear variation of a_0 broadly corresponds to the moderately relativistic range considered in this paper. For p-polarized light, PIC simulations show Brunel electrons injected into the plasma at each cycle of the laser pulse, bunched in space but with a spread of velocities [16].

We have also counted the number of electrons accelerated by the laser field and then reinjected back into the plasma. For that purpose, a very narrow plasma slab of width $0.1\lambda_L$ from the vacuum interface at $x = x_O$ was chosen, and the electron counts within that range were recorded during the laser pulse. Figure 5 plots electron counts $N(x_O,t)$ over the duration of a Gaussian pulse with pulse length $t_p = 10\,\tau_L$. The simulation was performed for the parameters $a_0 = 1.0$ and $n_{e0}/n_c = 20$.

D. Brunel excitation of the plasma line

As the electrons penetrate the overdense plasma they excite Langmuir waves. An estimate of the linear growth time of plasma oscillations t_g, for a beam of density n_b moving with velocity v_b, with a velocity spread Δv_b in a plasma of density

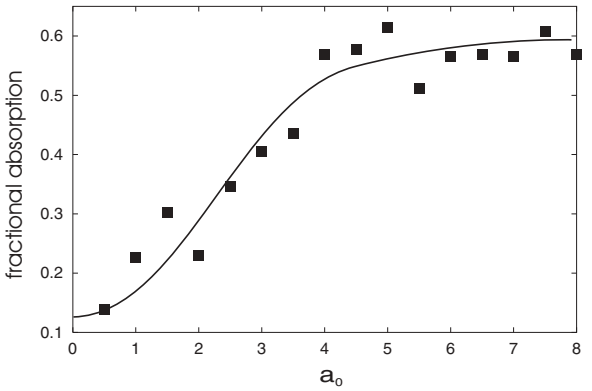

FIG. 4. Brunel absorption; fraction of energy deposited in the plasma as a function of $a_0 = 0.85(I_{18}\lambda_L^2)^{1/2}$. The data plotted are from PIC simulations and the line is a line of closest fit.

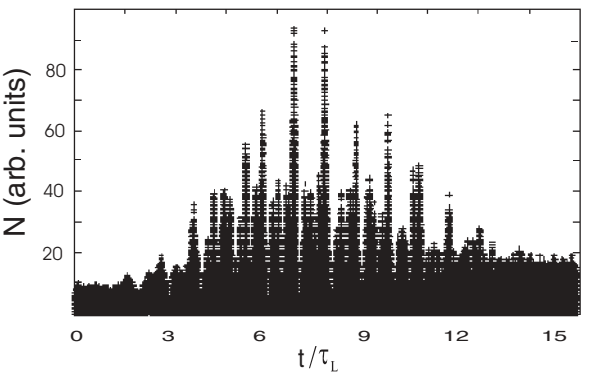

FIG. 5. Electron counts N as a function of t/τ_L for a pulse length $t_p = 10\,\tau_L$, for $a_0 = 1.0$ and $n_{e0}/n_c = 20$. Electrons were counted at $x = x_O$ close to the surface of the plasma box.

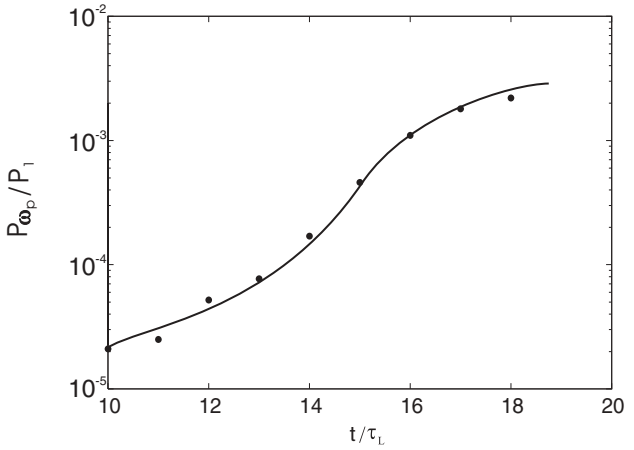

FIG. 6. Plasma emission conversion efficiency as a function of laser pulse length, for $a_0 = 2.0$ and $n_{e0}/n_c = 200$.

n_{e0} is $t_g \sim (n_c/n_b)\,(n_{e0}/n_c)^{1/2}\,(\Delta v_b/v_b)^2\,\tau_L$. At the intensities used in the simulations in Fig. 2, typically $(\Delta v_b/v_b) \sim 0.2$ which suggests a growth time of several laser periods. A linear estimate of the bandwidth of the Langmuir waves excited by the Brunel jets is $\Delta\omega \sim (\Delta v_b/v_b)\,(n_{e0}/n_c)^{1/2}\,\omega_L$, which is not inconsistent with the broadened plasma line detected in these runs.

Figure 6 plots PIC data showing the increase of the power emitted in the plasma line normalized to the incident laser power with time for the parameter choice $a_0 = 2.0$ and $n_{e0}/n_c = 200$. With this choice, Fig. 6 displays a sigmoid-shaped time dependence; for $t/\tau_L \lesssim 12$ growth is linear, evolving over a quasilinear central region before saturating.

To test the dependence of the growth of PLE on the velocity of the Brunel electrons, represented by $(\Delta v_b/v_b)^2$ in the estimate of linear growth, t_g, we carried out a set of simulations over a range of $a_0 = 0.5, 1.0, 2.0$ with $n_{e0}/n_c = 64$. Spectra were recorded over a range $5 \leqslant t_p/\tau_L \leqslant 50$. The evolution of the plasma line was followed to saturation. Table I shows saturation times for Langmuir growth, measured from the PIC runs, along with estimated (linear) growth times.

III. PARAMETRIC DEPENDENCE OF PLASMA EMISSION

In this section we consider further examples of Langmuir excitation over a range of pulse lengths from presaturation levels to saturation at longer pulse lengths. The evolution of the effect of plasma excitation is shown in Fig. 7 for the case $a_0 = 1.0$ and $n_{e0}/n_c = 80$ over three pulse lengths. Figure. 7(a) corresponds to relatively moderate Langmuir excitation, the principal manifestation being a modulation of harmonics on the blue side of the plasma resonance ($m_p \sim 9$), across a range $9 \leqslant m \leqslant 14$, approximately $0.5\,\omega_p$ in extent.

TABLE I. Estimates of PLE growth, $n_{e0}/n_c = 64$.

a_0	0.5	1.0	2.0
v_b/c	0.25	0.40	0.60
$t_g^{\rm est}/\tau_L$	2.5	2	1
$t_{\rm sat}^{\rm PIC}/\tau_L$	35	25	10

Further modulation cycles just above the threshold set earlier at $10^{-6}P_1$ span the range $14 \leqslant m \leqslant 18$ and $18 \leqslant m \lesssim 25$.

As the pulse length is increased, the identity of these features in Fig. 7(a) is lost as the intensities of harmonics are redistributed [Fig. 7(b)] while, for a pulse twice as long again, Langmuir growth has now saturated [Fig. 7(c)] with $P_{\omega_p}/P_1 \sim P_2/P_1$. The plasma line is now fully evolved and the spectrum assumes a structure akin to that in Fig. 2(a), showing fully evolved PLE, along with a modulation approximately $\Delta\omega/\omega_L \sim 5$ in extent. Figure 7(d) shows the PIC output for the three pulse lengths considered. On this evidence, modulation of the harmonic spectrum appears sensitive to the choice of pulse length, an issue we will return to in Sec. IV.

Relatively few PIC spectra were recorded using different pulse profiles. The limited set of data from these, somewhat contrary to expectations, suggested only a modest increase in the number of harmonics excited using a steepened pulse profile. More significant was a reduction in the PIC noise. Interestingly this characteristic of the PIC spectra mimics behavior in actual experiments. Von der Linde [32] reported clean harmonic spectra with little background noise in experiments where steeply rising pulses were used.

Figure 8 presents results from a set of runs for light of wavelength $\lambda_L = 1.054$ μm incident on a plasma box with initial density $n_{e0}/n_c = 75$. The pulse length $t_p/\tau_L = 10$ was chosen such that PLE is well below saturation. The intensity was varied across a range $0.5 \leqslant a_0 \leqslant 3.0$. For $a_0 = 0.5$, Fig. 8(a) shows around 13 harmonics with intensity above threshold, $P_m/P_1 = 10^{-6}$. Additionally, there is evidence of Langmuir wave excitation, already sufficiently intense to modulate the harmonic spectrum. Whereas low harmonics are unaffected, those in the range $9 \leqslant m \leqslant 14$ show the effects of plasma modulation. The inset in Fig. 8(a) shows the region of the spectrum in the neighborhood of the plasma frequency; line widths for harmonics on either side of the plasma frequency, though more particularly on the red side, show a distinctive broadening (typically $\Delta\omega/\omega_L \sim 0.3$).

When the laser intensity is increased ($a_0 = 1.0$), the range of harmonics above threshold now extends to $m_c = 23$ [cf. Fig. 8(b)], with a second modulation cycle apparent. Both m_c and the cycle of modulations extend further as a_0 is increased to 1.5 [cf. Fig. 8(c)]. However, as a_0 is increased beyond this, the corresponding increase in v_b ensures faster growth of PLE and the modulated harmonic structure changes conforming to the pattern found in Figs. 7(b) and 7(c). Figure 8(d) shows the growth in the number of harmonic lines excited above threshold across the range of a_0 considered.

Note that the modulated harmonic intensities in Fig. 8(c) show harmonic decay, m^{-p}, rather slower than decay indices in the range indicated by Gibbon's scaling law, where $3.5 \leqslant p \leqslant 6$. For the spectrum in Fig. 8(c), $p \sim 8/3$, coincident with the value proposed as a universal decay index by Baeva, Gordienko, and Pukhov [33].

Finally, we looked to see if there is any effect discernible from varying the electron temperature, T_e, on spectra with the plasma line present. Figure 9 shows spectra for the parameter set ($a_0 = 0.5$, $n_{e0}/n_c = 40$; $t_p/\tau_L = 30$) for light of wavelength $\lambda_L = 1.054$ μm for two values of electron temperature, $T_e = 0.1, 5.0$ keV. For $T_e = 5$ keV, peak power

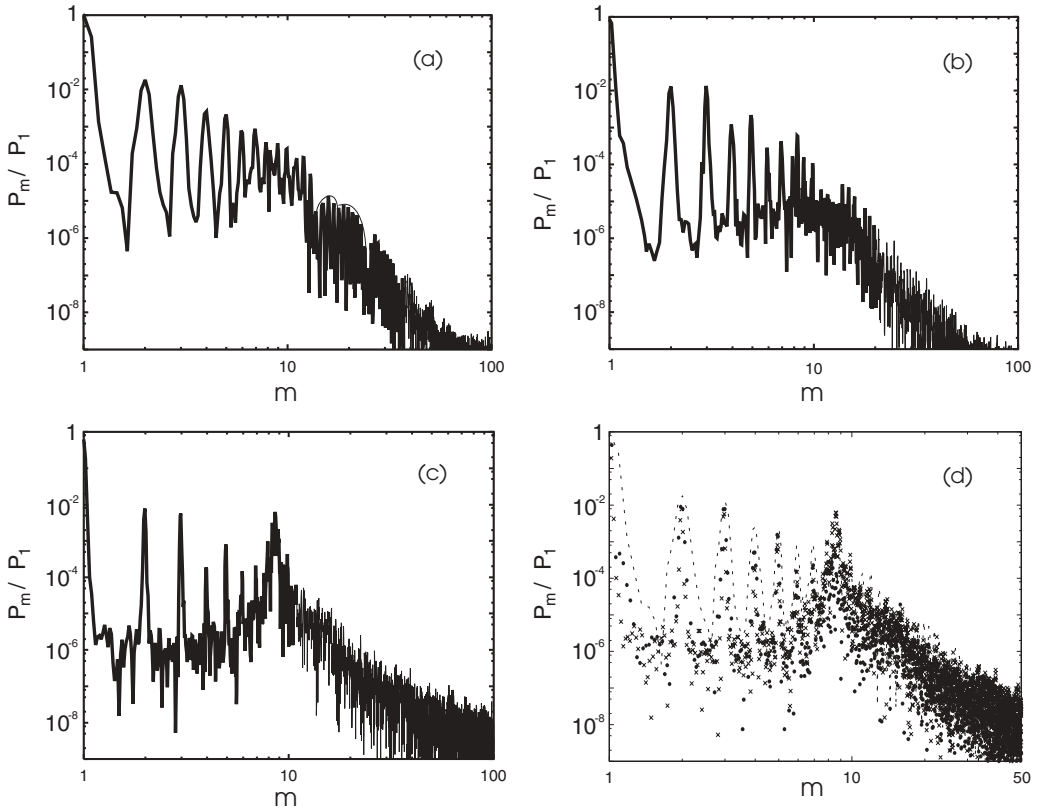

FIG. 7. Evolution of plasma emission as a function of pulse length from PIC runs with $a_0 = 1.0$ and $n_{e0}/n_c = 80$. (a) $t_p/\tau_L = 10$, (b) $t_p/\tau_L = 20$, (c) $t_p/\tau_L = 40$; (d) PIC data points for three pulse lengths superposed: $t_p/\tau_L = 10$ (dashed), 25 (•), and 40 (×).

radiated in the plasma line is reduced from its level for $T_e = 100$ eV by about a factor of 4.

In summary, we find that plasma effects on the high-harmonic spectrum are the outcome of a sensitive interplay between parameters characterizing the incident laser pulse (the peak intensity and duration of the pulse) and the target plasma (electron density and scale length). That sensitivity means that for any given combination of peak intensity and plasma density, along with the appropriate pulse length and scale length, it is not always easy to say precisely how the high-harmonic spectrum will be affected. By and large, for short pulses and relatively high electron densities, harmonics on the blue side of the plasma frequency showed signs of modulation at the plasma frequency. However, we saw [Fig. 7(c)] that as the pulse length increased, the high-harmonic spectrum in the neighborhood of m_p changed, with the emission of radiation at the plasma frequency and an attendant diminution in modulation in this region of the spectrum. Furthermore, it appears that modulation shows up most clearly in cases where the electron density chosen is such that ω_p is exactly resonant [as in Fig. 2(b)] or nearly so (Fig. 7). Figure 2(a) on the other hand corresponds to both a lower initial electron density and one that is not exactly resonant, differences that contribute to the observed differences in lineshapes.

A. Brunel-induced electron density structures

We saw in Sec. II that PIC simulations allow particle dynamics within the plasma to be tracked and collective bunching of the electrons to be observed as they move in the overdense plasma, close to the plasma-vacuum interface.

From these simulations a clear correlation was found between the reflected light and the sites of particle bunching with strong electrostatic fields within the plasma, identified as sources of emission. As we have emphasized already, the focus of our attention has been on the excitation of plasma oscillations at the peak electron density set initially for each PIC simulation. As a rule we disregarded plasma emission within the density ramp on the grounds that this was weaker by comparison. That notwithstanding, for times shorter than the saturation time for PLE, plasma emission is evident at electron densities within the ramp.

Figure 10 shows the statistics for electron counts across a plasma section $0.1\lambda_L$ wide, extending into the plasma from the plasma-vacuum interface. The parameters for this run were $a_0 = 0.5$ and $n_{e0}/n_c = 20$. The density ramp has a scale length $L/\lambda_L \sim 0.065$. In this run, the pulse length was such that PLE, though unsaturated, nevertheless shows up as the relatively strong electron peak at $k_L x = 3.54$. The peaks at $k_L x = 3.2, 3.32$ correspond to $n_{e0}/n_c = 4, 9$ respectively, and hence to plasma emission at $m = 2, 3$. However no peak in electron counts was registered at $k_L x = 3.46$ where $n_{e0}/n_c = 16$ and consequently no significant plasma emission is expected at $m = 4$.

B. Plasma line emission and coherent wake emission

That plasma emission from sites within the density ramp does contribute harmonics up to the plasma frequency

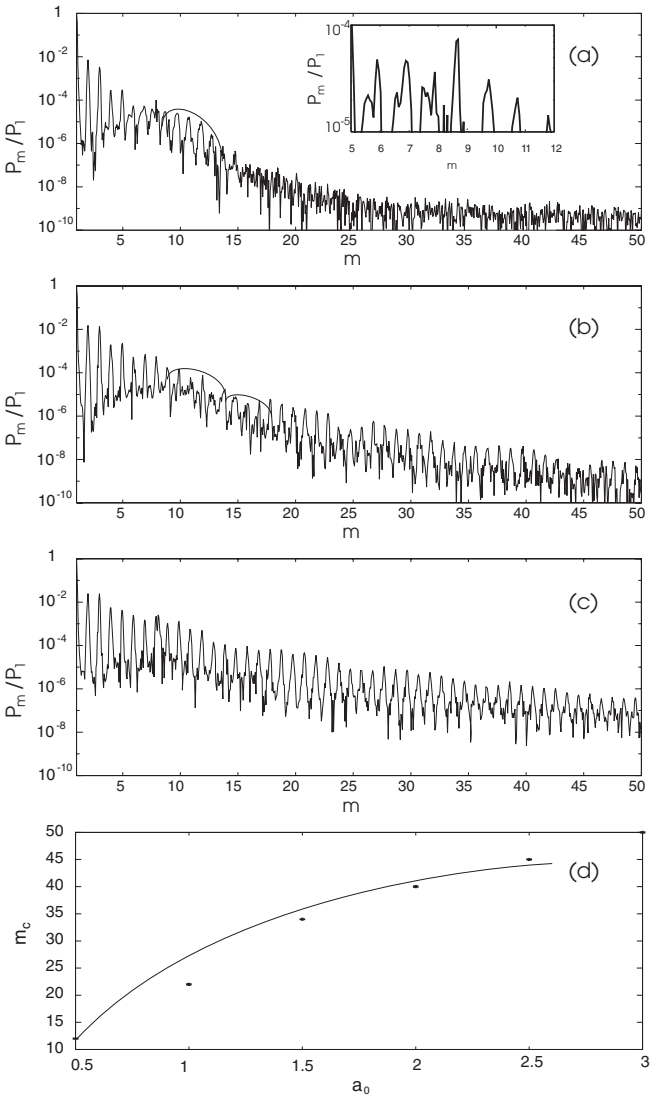

FIG. 8. Plasma emission growth and harmonic modulation as a function of laser intensity; (a) $a_0 = 0.5$, (b) $a_0 = 1.0$, (c) $a_0 = 1.5$, for $n_{e0}/n_c = 75$; (d) harmonic range m_c as a function of a_0.

corresponding to the peak electron density has been clearly established by Thaury and Quéré and their collaborators from observations of the reflected light, supplemented by PIC simulations [34,35]. Their work, which focused on a rather lower intensity range than that considered here, typically $a_0 \leqslant 0.2$, recorded spectra with low-order harmonics generated by plasma emission originating within the density ramp and scaling almost linearly with laser intensity. Thaury and Quéré termed this radiation *coherent wake emission*, CWE for short.

However, the mechanism which drives CWE is in reality no different from that responsible for the generation of PLE, described earlier by us [15,16]. The distinction between the two is largely one of emphasis. The focus of our work has been on PLE, and while Brunel-driven plasma emission at normalized frequencies up to $(n_{e0}/n_c)^{1/2}$ (as shown in Fig. 10) was clearly identified in our earlier work, plasma emission from within the density ramp was effectively masked by the

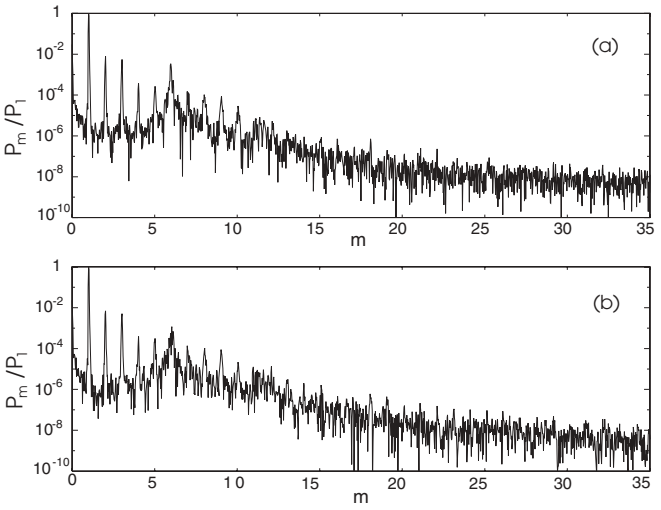

FIG. 9. Effects of temperature on plasma emission, $a_0 = 0.5$ and $n_{e0}/n_c = 40$, for (a) $T_e = 100$ eV and (b) $T_e = 5.0$ keV.

strength of low m harmonics driven by the $(\boldsymbol{v} \times \boldsymbol{B})$ source over the range of intensities investigated.

PLE, by contrast, for electron densities typical of most of our PIC simulations, appeared in a harmonic range over which intensities of the OMM harmonics had decreased by an order of magnitude or more from their $m = 2,3$ levels. In their work, Thaury and Quéré have drawn a distinction between two regimes, one in which harmonic generation is a consequence of CWE, the other being a fully relativistic regime where harmonics are generated by an oscillating mirror.

C. Evidence of plasma line emission from experiments

Plasma emission from laser-produced plasmas was first reported by Teubner *et al.* [36] and by von der Linde [32]. Teubner *et al.* identified a plasma line and a second harmonic, attributing the fundamental to surface emission and the harmonic to a source within the plasma where the plasma density was assumed to be lower on account of a lower degree of ionization. Teubner *et al.* held that the harmonic line should be stronger than the emission at the plasma frequency

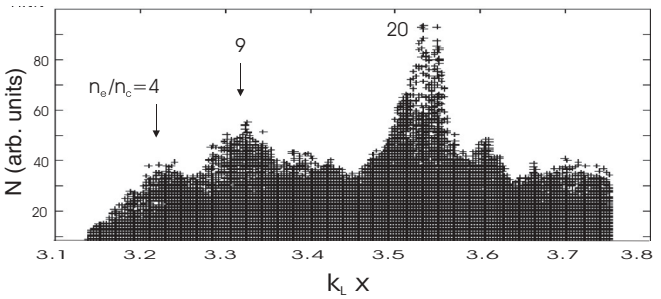

FIG. 10. Electron population inside the plasma during the laser-target interaction, for $a_0 = 0.5$, $n_{e0}/n_c = 20$, $\lambda_L = 0.248$ μm, and $t_p = 12$ fs. Density peaks correlate with $n_{e0}/n_c = 4, 9$ and 20. The plasma slice shown extends over $\Delta x = \lambda_L/10$ from the plasma-vacuum interface at a time $t = t_p$.

on grounds that the plasma line source is restricted to a thin surface layer.

However, in our simulations, the opposite appeared to hold, with the second harmonic typically 2–4 orders of magnitude weaker than the fundamental, though of course in these simulations we simply assume that $n_e(x,0) = n_{e0}$. Moreover the measured spectra show a frequency ratio between harmonic and fundamental of $\sim$1.6. Recalling that the feature centered at $\sim 1.5\,\omega_p$ in our PIC spectra when PLE is saturated is typically between 1 and 2 orders of magnitude more intense than the second harmonic, it is conceivable that what Teubner *et al.* identified as a surface plasma line and a harmonic emitted from within the plasma might alternatively be the plasma line and the combination line.

Von der Linde [32] reported strong plasma line emission around 20 nm and a feature at about 38 nm which appears in the spectrum between the harmonic lines $m = 20$ and $m = 23$; this he attributed to plasmon processes.

In the preceding section we made reference to the most complete characterization of plasma emission to date from the experiments of Thaury and Quéré *et al.* [34,35], focusing on the Brunel excitation of plasma oscillations across the density ramp, up to a cutoff at $m_c = (n_{e0}^{\max}/n_c)^{1/2}$ where $n_{e0}^{\max}$ denotes the peak electron plasma density. In these experiments, spectra were recorded using plastic, silica, aluminium, and gold targets. Across a spectral region that ranged from $\Delta m = 5$ in the case of plastic targets to around $\Delta m = 11$ for the other materials, remarkably uniform harmonics were resolved, with cutoffs at harmonic orders governed by the peak electron density in each instance. The relative intensity of PLE emission, by contrast, is no higher than a few percent of that of the lowest harmonic recorded, $m = 10$. In the spectra recorded in the experiments, individual harmonic lines are relatively broad, with $\Delta\omega \sim 0.2\,\omega_L$.

IV. PLASMA MODULATION OF HARMONIC SPECTRA

In this section, the modulation of the harmonic spectrum is characterized across a wider range of parameters than hitherto. As in the two preceding sections, how modulation characteristics depend on the intensity of the incident light and the density of the target plasma as well as on both the shape and length of the laser pulse, the nature of the density gradient at the front edge of the simulation plasma, and the electron temperature, is examined in detail.

A. Modulated spectra

In Ref. [19] we examined in detail the parametric dependence of the modulation on both the intensity of the incident light as well as on the plasma electron density. Broadly speaking, the higher the intensity, the more pronounced the modulation. At values of a_0 significantly below the range of interest (0.5–3.0), the number of harmonics with intensities above threshold (here set at 10^{-6}) is correspondingly reduced, a reduction reflected in the number of modulation cycles observed or indeed by their disappearance altogether. Since for the plasma model, the flux of Brunel electrons injected into the target plasma depends critically on intensity, a diminished flux means that the level of plasma waves excited in the overdense plasma is correspondingly weaker.

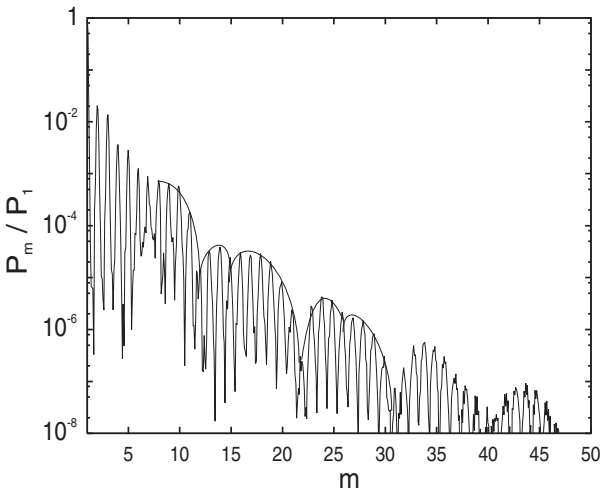

FIG. 11. Harmonic modulation for a laser pulse with $\tau = 17$ fs and $\lambda_L = 0.248\ \mu$m, for $a_0 = 0.5$ and $n_e 0/n_c = 60$. Envelopes over the harmonics have been added to indicate the respective modulation frequency.

In Ref. [19] we showed that across a range of densities $n_{e0} = 10n_c, 19n_c, 40n_c$, harmonic spectra showed three or four clear modulation cycles with average modulation frequencies $3.5\omega_L, 4.3\omega_L$, and $6.6\omega_L$, broadly corresponding to the plasma frequency in each case. There was, however, a hint of a harmonic substructure in the case of $n_e/n_c = 40$, underlying the modulation overall. A clearer view of this substructure is shown in Fig. 11 for a relatively weakly driven case, $a_0 = 0.5$ with $n_{e0}/n_c = 60$, for which $\omega_p \sim 7.8$. Plasma modulation is discernible on the blue side of the plasma frequency, extending to $m = 12$. For frequencies above this, the modulation shows fine structure with $\Delta m = 3$, followed by a plasma cycle extending to $m = 22$, beyond which harmonic intensities drop below threshold. This overall structure appears to be more common than one in which we find uniform modulation at the plasma frequency.

Figure 12 illustrates modulated spectra using pulses of different length incident on a plasma with relatively low density, $n_{e0}/n_c = 14$. We remarked in Sec. III that the degree of modulation in high-harmonic spectra appeared sensitive to the pulse length, an observation borne out by the spectra in Fig. 12, where the pulse length is varied from 17 to 41 fs. The number of cycles of modulation above threshold drops from 4 to 3 (at $t_p = 33$ fs) and as PLE saturates [Fig. 12(d)] is barely discernible. As we remarked in Sec. III, more steeply rising pulses resulted in less noisy spectra so that the definition of individual harmonics is improved. Otherwise, pulse shape appears to have little effect on the modulation.

Relaxing the steepness of the density gradient, on the other hand, has the effect of weakening the modulation. Whereas in the presence of a very steep density gradient the spectrum is uniformly modulated at $\Delta m = 4\omega_L$ [cf. Fig. 13(a)], for a choice of initial plasma scale length $L/\lambda_L \gtrsim 0.1$, intensity modulations are not evident in Fig. 13(b). This accords with an observation by Teubner *et al.* [17] and a similar conclusion reached in Ref. [37]. A more extensive ramp allows significant

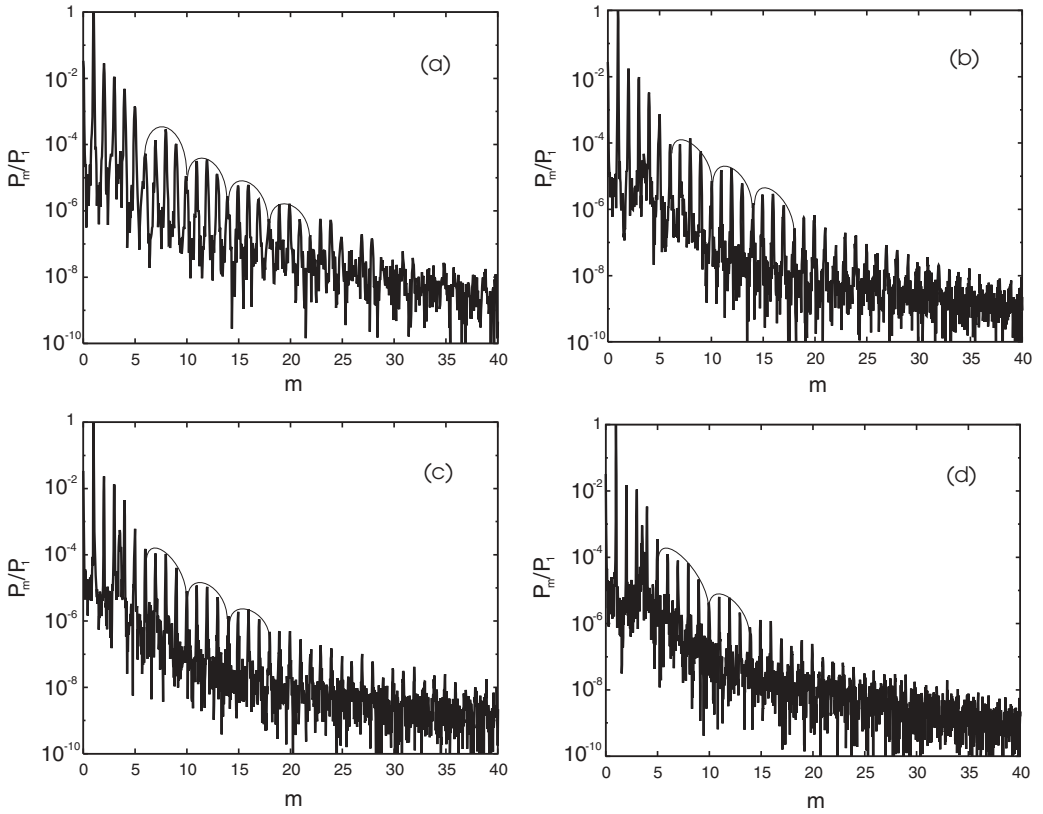

FIG. 12. Effect of pulse length on modulated harmonic emission, $a_0 = 0.5$ and $n_{e0}/n_c = 14$: (a) $t_p = 17$ fs, (b) $t_p = 25$ fs, (c) $t_p = 33$ fs, and (d) $t_p = 41$ fs.

Brunel excitation of plasma oscillations across the ramp. Thus, for example for the parameters used in Fig. 13(b), $n_{e0} = 16\,n_c$ and $a_0 = 0.6$, the simulations show enhanced emission at low harmonics, particularly for $m = 3$, consistent with additional plasma excitation at $n_{e0} = 9\,n_c$ in contrast to the sharp boundary case where only plasma oscillations with $\omega_p = 4\omega_L$ are present, with $m = 2,3$ ($\boldsymbol{v} \times \boldsymbol{B}$)-driven. The uniform modulation seen in Fig. 13(a) has all but disappeared in the presence of an extensive density ramp.

Finally, varying the electron temperature from 100 eV to 10 keV produced no marked effect on the modulation.

B. Experimental evidence of spectral modulation

Modulation, though comparatively commonplace in PIC-generated spectra, has not been widely reported in spectra recorded experimentally. In laboratory plasmas, some modulation of the harmonic spectrum was noted by Teubner *et al.* [17] in experiments using pulses typically 130 fs in duration, focused to intensities in the range $0.1 \leqslant I_{18} \lesssim 2.4$. Different target materials were used, notably aluminium, copper, glass, and silicated carbon. Across a harmonic range $5 \leqslant m \leqslant 22$ anomalies in emission were observed; in particular, there was a suggestion of modulation with $\Delta\,\omega \sim 2\,\omega_L$ in the case of a carbon target to around $4\,\omega_L$ for a glass target. No evidence of modulation was found in the spectra from metallic targets, a distinction attributed to differences in the enhancements of the electric field at the critical density. We note in passing that if there were grounds for assuming a more extensive underdense plasma in the case of metallic targets, then the absence of modulation in these cases would be consistent with our findings in Fig. 13. Teubner *et al.* appealed to the oscillating mirror model to interpret their observations, performing PIC simulations to support their contention that conditions at the critical surface were paramount in determining the harmonic structure observed. These comparisons showed overall discrepancies with the observed spectra. Notably the minima observed were not coincident with those found from the PIC model. While these experiments were characterized by clean experimental conditions, there was no clear indication of the actual plasma electron density, which makes comparison with PIC output uncertain.

In Ref. [19] we presented results of simulations in which $n_{e0}/n_c = 30$ and 45 alongside the harmonic efficiencies measured in Ref. [17] for carbon and glass targets using frequency-doubled light from a Ti:sapphire laser (of wavelength 395 nm) at an intensity 1.5×10^{18} W cm^{-2}. While comparisons of this kind can serve as little more than indications in view of the uncertainty over the electron densities in the plasmas created in the experiment, it was noted that in each case, the spectra, simulated and observed, showed a broadly comparable dependence on harmonic number. At the lower density, minima were observed at $m = 9,13$, corresponding exactly to those found by Teubner *et al.* for a carbon target, while for the higher density, these appeared at $m = 11,15$, consistent with those observed with a glass target.

To underline the pitfalls lurking in any comparison of PIC-generated spectra with the real thing, we show in Fig. 14 a

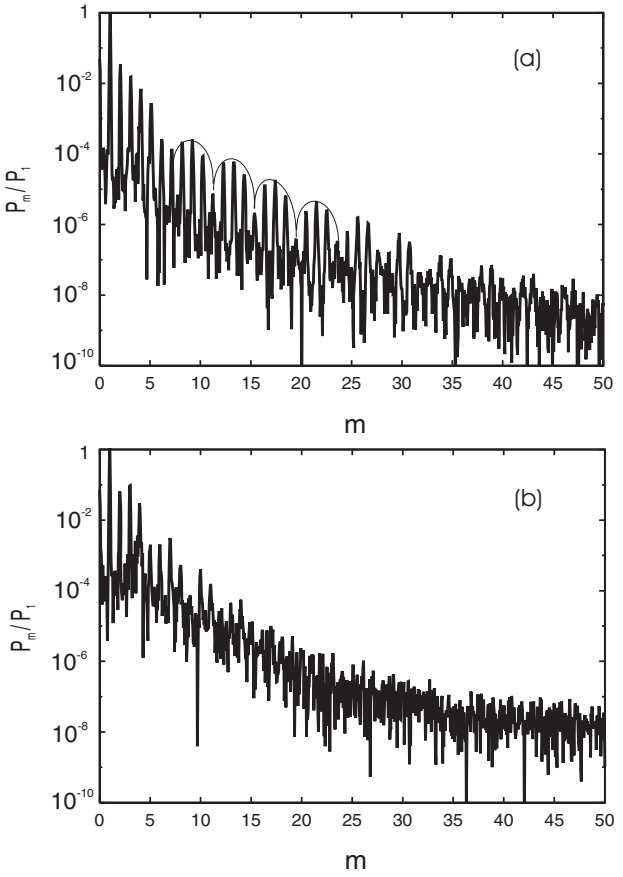

FIG. 13. Effect of density ramp on modulated harmonic emission, $a_0 = 0.6$ and $n_{e0}/n_c = 16$: (a) $\Delta x = 0.001\,\lambda_L$ and (b) $\Delta x = 0.2\,\lambda_L$.

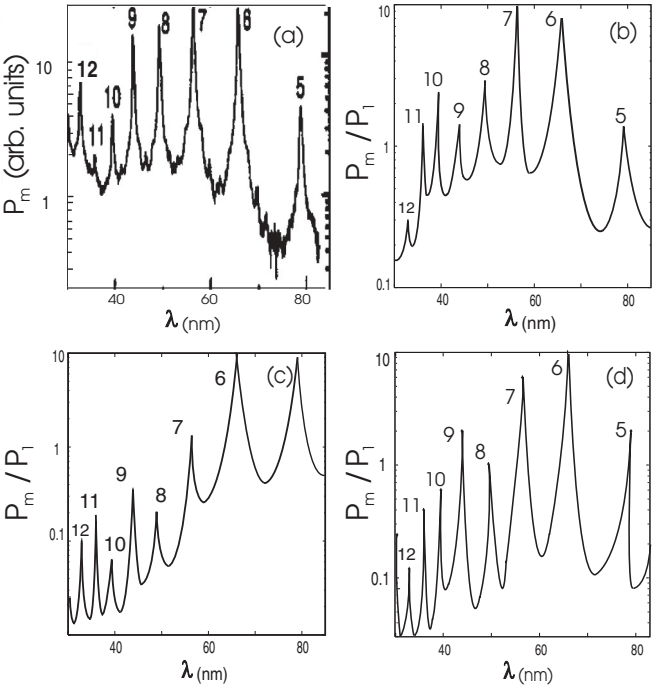

FIG. 14. (a) Modulation of the harmonic spectrum for a glass target irradiated with laser light of wavelength $\lambda_L = 0.395\ \mu$m and intensity corresponding to $a_0 = 0.4$ in pulses of 130 fs (Teubner *et al.* [17]); (b) PIC spectrum for $a_0 = 0.5$, $n_{e0}/n_c = 15$, and $t_p = 100$ fs; (c) PIC spectrum for $a_0 = 0.5$, $n_{e0}/n_c = 25$, and $t_p = 17$ fs; and (d) PIC spectrum for $n_{e0}/n_c = 30$, $t_p = 100$ fs, and $a_0 = 2.0$.

spectrum obtained by Teubner, Pretzler, Schlegel *et al.* from irradiating a glass target, together with PIC spectra from runs for different combinations of parameters. The measured spectrum shows harmonics from $m = 5$ to $m = 12$, with a minimum at $m = 11$, as well, presumably, as that at $m = 5$. On the short-wavelength side of this is plasma bremsstrahlung. Figures 14(b)–14(d) show the same spectral region from simulations with varying pulse lengths and choice of plasma electron densities. The variation among these highlights the difficulty inherent in attempting to compare the measured spectrum with PIC-generated spectra. The best match for the spectrum in Fig. 14(a) is with Fig. 14(d), though this is for an electron density higher than the maximum likely for a silicon glass target. Modulation is apparent in Fig. 14(d) with a band of three harmonics, followed by two bands of two harmonics, as compared to that found by Teubner *et al.* which shows two bands of three harmonics each. The spectrum in Fig. 14(b) is similar with a four-cycle band followed by one of three cycles. The short-pulse case in Fig. 14(c) presents a different pattern since now $m = 5$ coincides exactly with the initial plasma frequency, giving rise to modulation across harmonics $5 \leqslant m \leqslant 8$.

Spectra showing irregular modulation have been reported by Watts *et al.* [37]. Their results show modulation of (2–4)ω_L across a narrow range of harmonics ($20 \leqslant m \leqslant 33$), with conversion efficiencies greater than 10^{-6}. The structure observed in the spectrum was interpreted on the basis of the oscillating mirror model, in support of which Watts *et al.* appealed to PIC simulations that showed modulated harmonics, albeit at frequencies of (5–6)ω_L. Whether or not OMM is an appropriate model for interpreting spectral structure from these long-pulse experiments has been questioned (cf. Ref. [27]).

In making reference to these various observations, we emphasize again that, since electron densities in the source plasmas were not measured experimentally, the resulting uncertainty rules out an unequivocal identification of plasma effects as the source of the modulation observed. That notwithstanding, plasma modulation may play a role under favorable conditions. Given the incomplete state of our present understanding, it can hardly be dismissed out of hand.

V. CONCLUSIONS

In this paper we have examined the dependence of PLE not only on the incident laser intensity and plasma density, key parameters in any laser-plasma interaction, but on the duration and shape of the laser pulse as well as the density gradient and temperature of the plasma in question. The sensitive interplay among these various parameters determines whether or not plasma effects are likely to influence the high-harmonic spectrum, either as fully evolved PLE or, at an earlier phase, through the capacity of the growing plasma oscillation to modulate the spectrum. Whereas laser characteristics—intensity, pulse shape, and pulse length—are known, plasma characteristics in contrast are not. The plasma density profile and electron temperature are inferred rather than measured and

these uncertainties make for difficulty in attempting to draw comparisons between experiment and simulation.

We found that for short pulses, Langmuir growth is not saturated and the footprint of the plasma modification of the high-harmonic spectrum is a modulation of harmonics across a bandwidth $\Delta m\omega_L \gtrsim \omega_p$. However, for longer pulses, a strong plasma line evolves as a dominant feature in the harmonic spectrum. For steep plasma density profiles, the dominant plasma wave excited is at the peak electron density and so the modulation expected is at the corresponding plasma frequency. A combination of steep density profiles and relatively short pulse lengths appears to favor modulation at the plasma frequency, though at higher densities there is evidence of irregular modulation at multiple frequencies in place of several monochromatic cycles.

One of the pitfalls inherent in many simulations is the risk that output, while often seemingly plausible, may bear only limited relation to reality. Ideally, PIC simulations should go hand in hand with theory, but the difficulty in describing plasma emission in the context of laser-plasma interactions makes this a challenge that has not yet been met. There is no self-consistent theoretical model for the coupled excitation of plasma oscillations by Brunel electrons and their consequent coupling to the radiation field in the region of strong density gradients at the surface of target plasmas. What limited understanding that does exist in the range of moderately relativistic interactions has been pieced together from a mix of empirical models, PIC experiments and, less commonly, data from carefully designed experiments under well characterized experimental conditions. There is still some way to go in understanding the interplay between plasma excitation and the high harmonic spectrum, since we first drew attention to the effects of PLE in laser-plasma interactions.

ACKNOWLEDGMENTS

One of us (R.O.R.) acknowledges support from CONACyT under Contract No. 167185. T.J.M.B. acknowledges helpful exchanges with Professor Greg Tallents and with Dr. Paul Gibbon.

[1] N. H. Burnett, H. A. Baldis, M. C. Richardson, and G. D. Enright, Appl. Phys. Lett. **31**, 172 (1977).
[2] E. A. McLean, J. A. Stamper, B. H. Ripin, H. R. Griem, F. J. M. McMahon, and S. E. Bodner, Appl. Phys. Lett. **31**, 825 (1977).
[3] R. L. Carman, D. W. Forslund, and J. M. Kindel, Phys. Rev. Lett. **46**, 29 (1981).
[4] R. L. Carman, C. K. Rhodes, and R. F. Benjamin, Phys. Rev. A **24**, 2649 (1981).
[5] B. Bezzerides, R. D. Jones, and D. W. Forslund, Phys. Rev. Lett. **49**, 202 (1982).
[6] S. Kohlweyer, G. D. Tsakiris, C.-G. Wahlström, C. Tillman, and I. Mercer, Opt. Commun. **117**, 431 (1995).
[7] D. von der Linde, T. Engers, G. Jenke, P. Agostini, G. G. Grillon, E. Nibbering, A. Mysyrowicz, and A. Antonetti, Phys. Rev. A **52**, R25 (1995).
[8] P. A. Norreys, M. Zepf, S. Moustaizis, A. P. Fews, J. Zhang, P. Lee, M. Bakarezos, C. N. Danson, A. Dyson, P. Gibbon, P. Loukakos, D. Neely, F. N. Walsh, J. S. Wark, and A. E. Dangor, Phys. Rev. Lett. **76**, 1832 (1996).
[9] P. Gibbon, Phys. Rev. Lett. **76**, 50 (1996).
[10] S. C. Wilks, W. L. Kruer, and W. B. Mori, IEEE Trans. Plasma Sci. **21**, 120 (1993).
[11] W. L. Kruer, *The Physics of Laser Plasma Interactions* (Addison-Wesley, New York, 1988).
[12] S. V. Bulanov, N. M. Naumova, and F. Pegoraro, Phys. Plasmas **1**, 745 (1994).
[13] R. Lichters, J. Meyer-ter-Vehn, and A. Pukhov, Phys. Plasmas **3**, 3425 (1997).
[14] D. von der Linde and K. Rzążewski, Appl. Phys. B **63**, 499 (1996).
[15] R. Ondarza-Rovira and T. J. M. Boyd, in *Proceedings of the International Conference on Plasma Physics, Nagoya, 1996*, edited by H. Sugai and T. Hayashi (Japan Society of Plasma Science in Nuclear Fusion Research, Nagoya, 1997), Vol. 2, p. 1718; R. Ondarza-Rovira, Ph.D. thesis, University of Essex, 1996.
[16] T. J. M. Boyd and R. Ondarza-Rovira, Phys. Rev. Lett. **85**, 1440 (2000).
[17] U. Teubner, G. Pretzler, Th. Schlegel, K. Eidmann, E. Förster, and K. Witte, Phys. Rev. A **67**, 013816 (2003).
[18] T. J. M. Boyd and R. Ondarza-Rovira, in *Proceedings of the Inertial Fusion Sciences and Applications, Biarritz, France, 2005*, edited by J.-C. Gauthier, B. Hammel, H. Azechi, and C. Labaune (EDP Sciences, Les Ulis, France, 2006) [J. Phys. IV (France) **133**, 479 (2006)].
[19] T. J. M. Boyd and R. Ondarza-Rovira, Phys. Rev. Lett. **98**, 105001 (2007).
[20] N. Ben-Yosef and A. S. Kaufman, Electron. Lett. **2**, 175 (1966).
[21] W. Bernstein, F. F. Chen, M. A. Heald, and A. Z. Kranz, Phys. Fluids **1**, 430 (1958).
[22] P. A. Forsyth, W. Petrie, and B. W. Currie, Can. J. Phys. **28**, 324 (1950).
[23] J. P. Wild, J. D. Murray, and W. C. Rowe, Nature (London) **172**, 533 (1953).
[24] V. L. Ginzburg and V. V. Zheleznyakov, Soviet Astron. AJ. **2**, 653 (1958); J. P. Wild, S. F. Smerd, and A. A. Weiss, Annu. Rev. Astron. Astrophys. **1**, 291 (1963); D. B. Melrose, *Instabilities in Space and Laboratory Plasmas* (Cambridge University Press, Cambridge, UK, 1986).
[25] T. J. M. Boyd, D. A. Tidman, and T. H. Dupree, University of Maryland Technical Note No. BN-287, 1962 (unpublished); Phys. Fluids **8**, 1860 (1965); D. B. Melrose, Space Sci. Rev. **26**, 3 (1980).
[26] H. C. Barr, T. J. M. Boyd, G. A. Gardner, and R. Rankin, Phys. Fluids **28**, 16 (1985).
[27] U. Teubner and P. Gibbon, Rev. Mod. Phys. **81**, 445 (2009).
[28] A. Bourdier, Phys. Fluids **26**, 1804 (1983).
[29] F. Brunel, Phys. Rev. Lett. **59**, 52 (1987).
[30] P. Gibbon, *Short Pulse Laser Interactions with Matter. An Introduction* (Imperial College Press, London, 2005).
[31] J. R. Davies, Plasma Phys. Control. Fusion **51**, 014006 (2009).
[32] D. von der Linde, Appl. Phys. B **68**, 315 (1999).

[33] T. Baeva, S. Gordienko, and A. Pukhov, Phys. Rev. E **74**, 065401 (2006).

[34] F. Quéré, C. Thaury, P. Monot, S. Dobosz, Ph. Martin, J.-P. Geindre, and P. Audebert, Phys. Rev. Lett. **96**, 125004 (2006).

[35] C. Thaury and F. Quéré, J. Phys. B: At. Mol. Opt. Phys. **43**, 213001 (2010).

[36] U. Teubner, D. Altenbernd, P. Gibbon, E. Förster, A. Mysyrowicz, P. Audebert, J.-P. Geindre, J. C. Gauthier, R. Lichters, and J. Meyer-ter-Vehn, Opt. Comm. **144**, 217 (1997).

[37] I. Watts, M. Zepf, E. L. Clark, M. Tatarakis, K. Krushelnick, A. E. Dangor, R. M. Allott, R. J. Clarke, D. Neely, and P. A. Norreys, Phys. Rev. Lett. **88**, 155001 (2002).